



Missouri University of Science and Technology  
Scholars' Mine

---

International Specialty Conference on Cold-Formed Steel Structures

(2014) - 22nd International Specialty Conference on Cold-Formed Steel Structures

---

Nov 5th, 12:00 AM - 12:00 AM

## Shape Optimisation of Cold-Formed Steel Profiles with Manufacturing Constraints - Part II: Applications

Bin Wang

Benoit P. Gilbert

Adrien M. Molinier

Hong Guan

Lip H. Teh

Follow this and additional works at: <https://scholarsmine.mst.edu/isccss>

 Part of the [Structural Engineering Commons](#)

---

### Recommended Citation

Wang, Bin; Gilbert, Benoit P.; Molinier, Adrien M.; Guan, Hong; and Teh, Lip H., "Shape Optimisation of Cold-Formed Steel Profiles with Manufacturing Constraints - Part II: Applications" (2014). *International Specialty Conference on Cold-Formed Steel Structures*. 3.

<https://scholarsmine.mst.edu/isccss/22iccfss/session01/3>

This Article - Conference proceedings is brought to you for free and open access by Scholars' Mine. It has been accepted for inclusion in International Specialty Conference on Cold-Formed Steel Structures by an authorized administrator of Scholars' Mine. This work is protected by U. S. Copyright Law. Unauthorized use including reproduction for redistribution requires the permission of the copyright holder. For more information, please contact [scholarsmine@mst.edu](mailto:scholarsmine@mst.edu).

## **Shape optimisation of cold-formed steel profiles with manufacturing constraints - Part II: Applications**

Bin Wang<sup>1</sup>, Benoit P. Gilbert<sup>2</sup>, Adrien M. Molinier<sup>3</sup>, Hong Guan<sup>4</sup>, Lip H. Teh<sup>5</sup>

### **Abstract**

This paper uses the Genetic Algorithm (GA)-based optimisation method for cold-formed steel (CFS) profiles with manufacturing constraints, developed in the companion paper, to shape-optimize simply-supported and singly-symmetric open-section columns. Having a uniform wall thickness of 0.047 inch (1.2 mm), the columns are subjected to a compressive axial load of 16,860 lbf (75kN) and optimized for yielding and global buckling. Column lengths ranging from 3.28 ft (1,000 mm) to 9.84 ft (3,000 mm) are investigated. The algorithm is run with and without considering the manufacturing constraints. Differences between the two types of cross-sections, i.e. manufacturable and non-manufacturable, are evaluated. The influence of the number of manufacturable flat segments on the optimized cross-sectional area is also investigated. Future developments of the method for strength optimisation under combined actions and practical applications are discussed.

---

<sup>1</sup> PhD Candidate, Griffith School of Engineering, Griffith University, Australia (b.wang@griffith.edu.au)

<sup>2</sup> Senior Lecturer, Griffith School of Engineering, Griffith University, Australia (b.gilbert@griffith.edu.au)

<sup>3</sup> Exchange undergraduate student, Griffith School of Engineering, Griffith University, Australia

<sup>4</sup> Associate Professor, Griffith School of Engineering, Griffith University, Australia (h.guan@griffith.edu.au)

<sup>5</sup> Senior Lecturer, School of Civil, Mining and Environmental Engineering, University of Wollongong, Australia (lteh@uow.edu.au)

## 1. Introduction

In this paper, the applications of the validated algorithm for shape optimisation of CFS profiles with manufacturing constraints, developed in the companion paper (Wang et. al., 2014), are investigated. The singly-symmetric open cross-sectional shapes of free to warp and simply-supported columns are optimised. Column lengths of 3.28 ft (1,000 mm), 6.56 ft (2,000 mm) and 9.84 ft (3,000 mm) are investigated. For simplicity, only yielding and global buckling modes are considered herein. The algorithm is run with and without considering the manufacturing constraints, and the paper compares the two types of optimised cross-sections. The influence of the number of manufacturable flat segments on the optimised cross-sections is also investigated. Future developments of the method for strength optimisation under combined actions and practical applications are discussed.

## 2. Optimisation problem

The optimisation problem consists of minimising the cross-sectional area  $A_s$  of free to warp, simply-supported and singly-symmetric open-section CFS columns subjected to an axial compressive force  $N^*$  of at least 16,861 lbf (75 kN). The columns have an uniform wall thickness  $t$  of 0.047 inch (1.2 mm). The yield stress  $f_y$  of the column is equal to 65 psi (450 MPa), the Young's modulus  $E$  to 29,000 ksi (200 GPa) and the shear modulus  $G$  to 11,600 ksi (80 GPa). The optimisation problem is illustrated in Fig. 1.

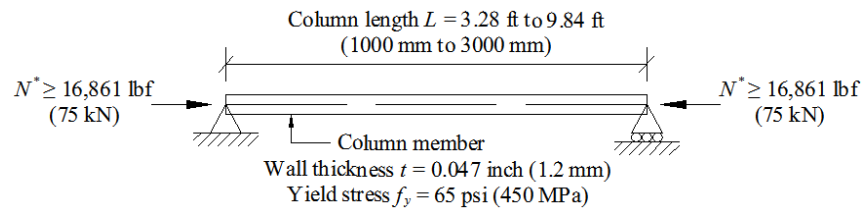


Fig. 1. Optimisation problem

The manufacturing constraints defined in the companion paper (Wang et. al., 2014) are introduced into the Genetic Algorithm (GA)-based shape optimisation algorithm for singly-symmetric open cross-sections developed in (Gilbert et. al., 2012a).

The unconstrained optimisation problem, suitable for GA, consists of minimising the fitness function  $f$ ,

$$f = \frac{A_s}{A_{squash}} + \alpha_x \max\left(0, \frac{N^*}{N_c} - 1\right) + \alpha_{align} \omega \left| \frac{nbAligned}{nbElement} - 1 \right| \quad (1)$$

where  $N_c$  is the nominal compressive axial capacity for global buckling, calculated based on the Australian standard AS/NZS 4600 (2005), and  $\alpha_x$  and  $\alpha_{align}$  are penalty factors. The variables  $\omega$ ,  $nbAligned$  and  $nbElement$  refer to the alignment equality constraint and are defined in the companion paper (Wang et. al., 2014). A value of  $\omega = 0.5$  is used herein. The constraint on the axial capacity is expressed as an inequality constraint. The squash area  $A_{squash}$  is defined as the lower bound cross-sectional area of the profile and is expressed as,

$$A_{squash} = \frac{N^*}{f_y} \quad (2)$$

The Augmented Lagrangian (AL) method for GA proposed by Adeli and Cheng (1994) is used to handle the axial capacity and manufacturing constraints. The fitness function  $f$  is then expressed as,

$$f = \frac{A_s}{A_{squash}} + \frac{1}{2} \left\{ \gamma_x \left[ \max\left(0, \frac{N^*}{N_c} - 1 + \mu_x\right) \right]^2 + \gamma_{align} \left[ \omega \left| \frac{nbAligned}{nbElement} - 1 \right| + \mu_{align} \right]^2 \right\} \quad (3)$$

where the AL parameters are defined in Section 4.1 of the companion paper (Wang et. al., 2014). Initial values of  $\gamma_x$  and  $\gamma_{align}$  are set to 2 and 0.1, respectively (Wang et. al., 2014).

For all column lengths, the design space is set to 3.937 inch  $\times$  3.937 inch (100 mm  $\times$  100 mm) (Gilbert et. al., 2012a) and the maximum number of generations to 300 per run. 10 runs are performed for each optimisation problem to find (i) optimised manufacturable (i.e. with manufacturing constraints) and (ii) non-manufacturable (i.e. without manufacturing constraints) cross-sections. The number of individuals per generation is set to 500 and the cross-sections are drawn with elements of nominal length of 0.158 inch (4 mm) (see Gilbert et. al. (2012a, b) for more details). The probabilities of cross-over and mutation operations for the GA are equal to 80% and 5%, respectively, as recommended in (Gilbert et. al., 2012b). As the cross-sections of interest are singly-symmetric, only half of the cross-sections is optimised.

For the Hough transformation, used to detect flat segments in the cross-sections (see the companion paper (Wang et. al., 2014)), values of  $\Delta\theta = 1^\circ$  and alignment

tolerance  $\Delta r = 2t$  (i.e. twice the wall thickness) are used as a compromise between accuracy and computational time (about 3, 6 and 10 hours per run for the 3.28 ft (1,000 mm), 6.56 ft (2,000 mm) and 9.84 ft (3,000 mm) long columns, respectively, on a 792 core HPC cluster consisting of a mixture of SGI Altix XE and SGI® Rackable™ C2114-4TY14 servers at Griffith University, Australia).

To study the influence of the maximum number of discrete bends on the optimised cross-sectional shape, various maximum numbers of flat segments  $N_{max}$  per half cross-section are investigated. Specifically,  $N_{max}$  is set to 3, 4, 5 and 6 for 3.28 ft (1,000 mm), 4, 5, 6 and 7 for 6.56 ft (2,000 mm), and 5, 6, 7 and 8 for 9.84 ft (3,000 mm) long columns.

### 3. Determination of the nominal axial compressive capacity $N_c$

The nominal axial compressive member capacity  $N_c$  for flexural and flexural-torsional buckling (global buckling), is given in the CFS Australian standard AS/NZS 4600 (2005) as,

$$\text{if } \lambda_c \leq 1.5, N_c = (0.658^{\lambda_c}) N_y \quad (4)$$

$$\text{if } \lambda_c > 1.5, N_c = \left( \frac{0.877}{\lambda_c^2} \right) N_y \quad (5)$$

where  $N_y$  is the nominal yield compressive capacity, calculated as the product of the cross-sectional area  $A_s$  and yield stress  $f_y$  (i.e.  $N_y = f_y A_s$ ). The variable  $\lambda_c$  is a non-dimensional slenderness ratio defined as,

$$\lambda_c = \sqrt{\frac{f_y}{f_{oc}}} \quad (6)$$

where  $f_{oc}$  is the least of the elastic flexural buckling stress  $f_{oy}$  about the  $y$ -axis (i.e. perpendicular to the symmetric  $x$ -axis) and the flexural-torsional buckling stress  $f_{oxz}$ . These buckling stresses are expressed as,

$$f_{oy} = \frac{\pi^2 E}{(l_{ey}/r_y)^2} \quad (7)$$

$$f_{oxz} = \frac{1}{2\beta} \left[ (f_{ox} + f_{oz}) - \sqrt{(f_{ox} + f_{oz})^2 - 4\beta f_{ox} f_{oz}} \right] \quad (8)$$

where  $f_{ox}$  is the elastic flexural buckling stress about the symmetric  $x$ -axis,  $f_{oz}$  is the elastic torsional buckling stress about the longitudinal  $z$ -axis, and  $\beta$  is a coefficient. These variables are given as,

$$f_{ox} = \frac{\pi^2 E}{(l_{ex}/r_x)^2} \quad (9)$$

$$f_{oz} = \frac{GJ \left( 1 + \pi^2 EC_w / GJ l_{ez}^2 \right)}{A_s r_{ol}^2} \quad (10)$$

$$\beta = 1 - \left( \frac{x_{os}}{r_{ol}} \right)^2 \quad (11)$$

where  $J$  is the St-Venant torsion constant,  $C_w$  is the warping constant,  $r_x$  and  $r_y$  are the radii of gyration about the  $x$ - and  $y$ -axes, respectively,  $l_{ex}$ ,  $l_{ey}$  and  $l_{ez}$  are the effective lengths for buckling about  $x$ -,  $y$ - and  $z$ -axes, respectively,  $x_{os}$  is the distance between the shear centre and the centroid, and  $r_{ol}$  is the polar radius of gyration of the cross section defined as,

$$r_{ol} = \sqrt{\frac{I_x + I_y}{A_s} + x_{os}^2} \quad (12)$$

## 4. Results and discussion

### 4.1. Column length of 3.28 ft (1,000 mm)

Fig. 2 depicts the average fitness functions  $f$  given in Eq. (1) over 10 runs, with penalty factors  $\alpha_x = \alpha_{align} = 10$  for the manufacturable cross-sections and  $\alpha_x = 10$  for the non-manufacturable one, for the 3.28 ft (1,000 mm) long columns. When the algorithm is run with manufacturing constraints, the algorithm converges slower to the optimised cross-section when  $N_{max} = 3$  than when  $N_{max} > 3$ . The optimised cross-section with  $N_{max} = 3$  is composed of longer flat segments than when  $N_{max} > 3$  and it is more difficult for the algorithm to align elements in the Hough transformation. For the  $N_{max} > 3$  curves, the convergence trend seems to be similar, likely because the algorithm approaches the optimised solution with only four flat segments per half cross-section. For the non-manufacturable cross-

section (referred to as  $N_{max} = 0$  herein), the algorithm converges the fastest.

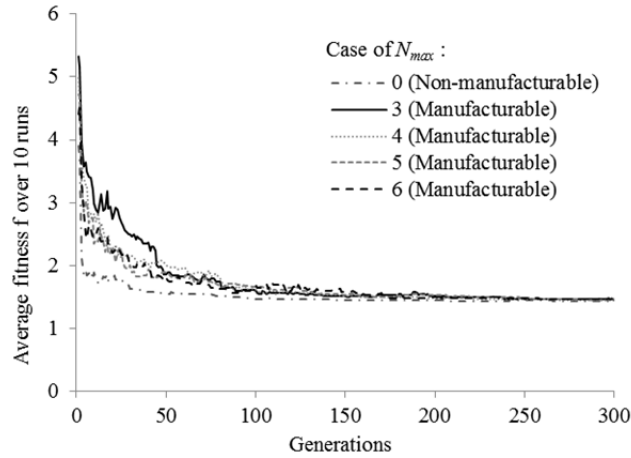


Fig. 2. Average fitness  $f$  for the 3.28 ft (1,000 mm) long columns

$N_{max}$	Cross-sectional area	Compression capacity			Alignment	
	$A_s$ (inch <sup>2</sup> (mm <sup>2</sup> ))	$N_c$ (lbf (kN))	Error <sup>(2)</sup> (%)	CoV	Error (%)	CoV
0 <sup>(1)</sup>	0.3694 (238.3)	16874 (75.06)	+0.09	0.0012	-	-
3	0.3739 (241.2)	16872 (75.05)	+0.07	0.0016	0.0	0.0000
4	0.3711 (239.4)	16865 (75.02)	+0.03	0.0015	0.0	0.0000
5	0.3706 (239.1)	16883 (75.10)	+0.14	0.0015	0.0	0.0000
6	0.3708 (239.2)	16892 (75.14)	+0.19	0.0023	0.0	0.0000

<sup>(1)</sup>: Algorithm ran without manufacturing constraints (non-manufacturable cross-section)

<sup>(2)</sup>: Error when compared to 75 kN

Table 1. Average results over 10 runs for the 3.28 ft (1,000 mm) long columns

Table 1 summarises the average results over 10 runs. When the algorithm is run with manufacturing constraints, the algorithm always satisfies the alignment constraint. The algorithm also always satisfies an average compressive axial capacity of at least 16,861 lbf (75 kN). Specifically, 6, 6, 8 and 7 runs out of 10 satisfy all constraints when  $N_{max} = 3, 4, 5$  and  $6$ , respectively. For the non-manufacturable cross-section, the constraint is satisfied for 8 runs out of 10. The case  $N_{max} = 5$  provides the smallest average cross-sectional area of 0.3708 inch<sup>2</sup> (239.1 mm<sup>2</sup>). This is 0.34% greater than the average non-manufacturable optimised cross-sectional area of 0.3694 inch<sup>2</sup> (238.3 mm<sup>2</sup>).

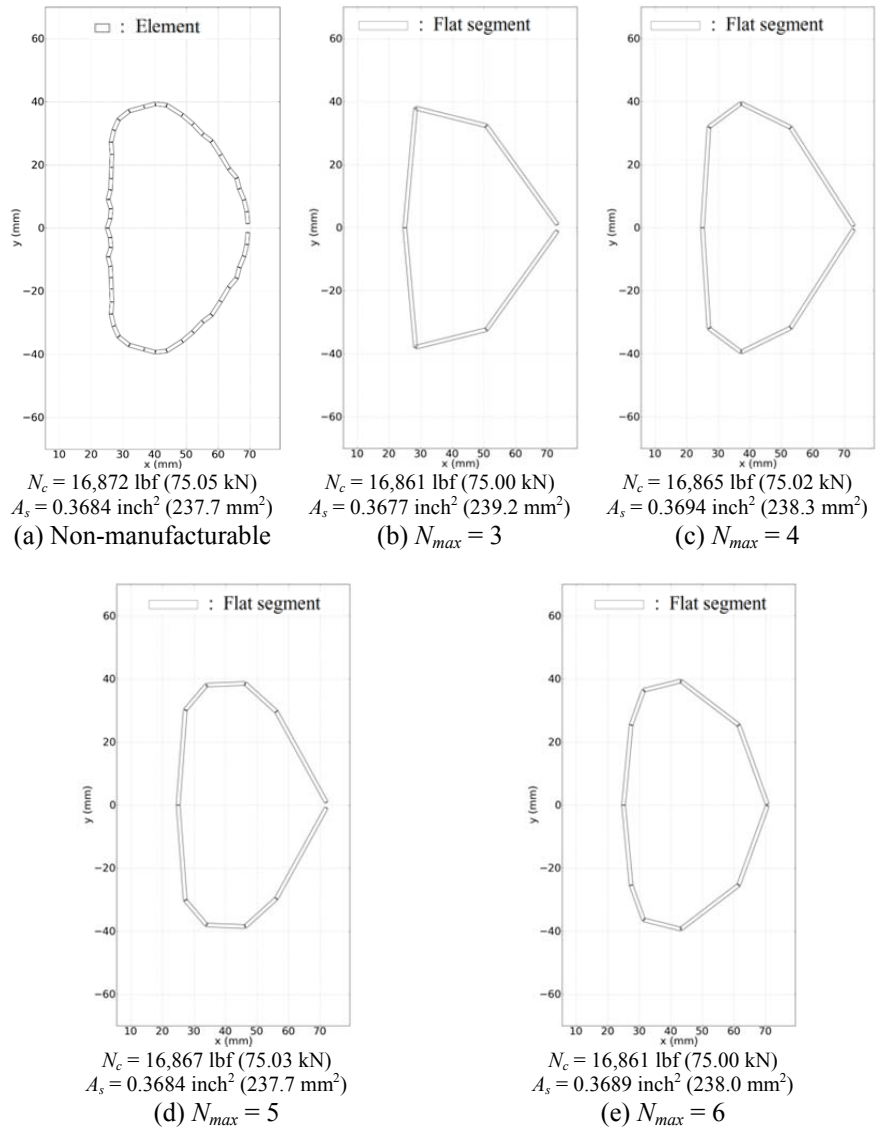


Fig. 3. Fittest optimised cross-sections for the 3.28 ft (1,000 mm) long columns at the final generation for (a) the non-manufacturable cross-section and (b) to (e)  $N_{max} = 3$  to 6



Fig. 3 plots the optimised fittest cross-sections at the 300<sup>th</sup> generation (final generation) out of 10 runs for each case investigated, i.e. non-manufacturable cross-section and  $N_{max} = 3$  to 6. The fittest cross-section is defined as the one satisfying all constraints and with the smaller cross-sectional area out of the 10 runs. The figure shows that all cross-sections tend to converge to a “bean” shape with an overall depth of about 3.150 inch (80 mm). When  $N_{max}$  increases, the algorithm mainly tends to subdivide the flat segments further away from the axis of symmetry. This “rounds” the cross-sectional shape at this location to best match the optimised non-manufacturable cross-sectional shape, shown in Fig. 3 (a). As shown in Fig. 3 (d, e) and Table 1, five flat segments ( $N_{max} = 5$ ) per half cross-section seems to be sufficient to best match the optimised non-manufacturable cross-sectional shape and likely represents an optimum number of flat segments for column lengths of 3.28 ft (1,000 mm).

#### 4.2. Column length of 6.56 ft (2,000 mm)

Similar to Fig. 2, Fig. 4 depicts the average fitness functions  $f$  over 10 runs for the 6.56 ft (2,000 mm) long columns. Similar observations to Section 4.1 can be made and the more the number of flat segments, the faster the convergence of the algorithm. For the  $N_{max} > 4$  curves, the convergence trend seems to be similar, and likely a minimum of five flat segments per half cross-section are needed to approach the optimum solution. The algorithm also converges the fastest when manufacturing constraints are ignored ( $N_{max} = 0$ ).

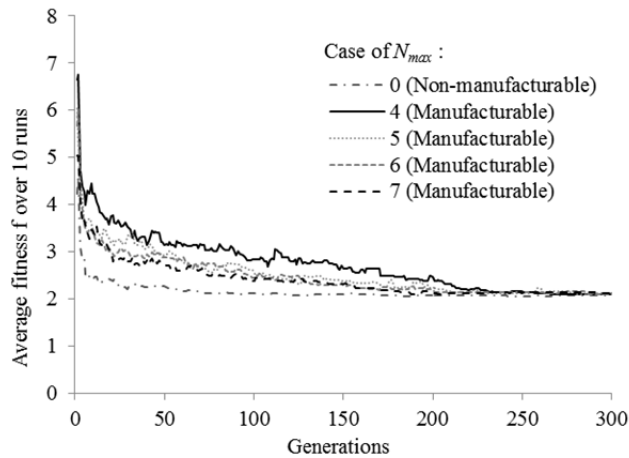


Fig. 4. Average fitness  $f$  for the 6.56 ft (2,000 mm) long columns

$N_{max}$	Cross-sectional area	Compression capacity			Alignment	
	$A_s$ (inch <sup>2</sup> (mm <sup>2</sup> ))	$N_c$ (lbf (kN))	Error <sup>(2)</sup> (%)	CoV	Error (%)	CoV
0 <sup>(1)</sup>	0.5281 (340.7)	16906 (75.20)	+0.20	0.0044	-	-
4	0.5310 (342.6)	16930 (75.31)	+0.41	0.0061	0.0	0.0000
5	0.5293 (341.5)	16971 (75.49)	+0.65	0.0096	0.0	0.0000
6	0.5296 (341.7)	16870 (75.04)	+0.06	0.0062	0.0	0.0000
7	0.5289 (341.2)	16944 (75.37)	+0.49	0.0076	0.0	0.0000

<sup>(1)</sup>: Algorithm ran without manufacturing constraints (non-manufacturable cross-section)

<sup>(2)</sup>: Error when compared to 75 kN

Table 2. Average results over 10 runs for the 6.56 ft (2,000 mm) long columns

Table 2 summarises the average results over 10 runs. When the algorithm is run with manufacturing constraints, the algorithm always satisfies the alignment constraint. The algorithm also always satisfies an average compressive axial capacity of at least 16,861 lbf (75 kN). Specifically, 6, 9, 5 and 7 runs out of 10 satisfy all constraints when  $N_{max} = 4, 5, 6$  and  $7$ , respectively. For the non-manufacturable cross-section, the constraint is satisfied for 9 runs out of 10. The case  $N_{max} = 7$  provides the smallest average cross-sectional area of 0.5289 inch<sup>2</sup> (341.2 mm<sup>2</sup>). This is 0.15% greater than the average optimised non-manufacturable cross-sectional area of 0.5281 inch<sup>2</sup> (340.7 mm<sup>2</sup>).

Fig. 5 plots the optimised fittest cross-sections at the 300<sup>th</sup> generation (final generation) out of 10 runs for each investigated case, i.e. non-manufacturable cross-section and  $N_{max} = 4$  to  $7$ . The figure shows that all cross-sections tend to converge to a “bean” shape with an overall depth of about 4.528 inch (115 mm). The optimised manufacturable cross-sections also tend to be wider (about 2.559 to 2.756 inch (65 to 70 mm)) than the non-manufacturable optimised cross-section (about 2.362 inch (60 mm)). The fittest cross-section, shown in Fig. 5 (e), is for  $N_{max} = 7$ . Yet, per half cross-section, it has two flat segments in the “web” and two flat segments in the “lip” that are nearly aligned. Moreover, it has (i) a similar cross-sectional shape to the fittest cross-section ( $N_{max} = 5$  in Fig. 5 (c)) and (ii) a cross-sectional area of only 0.03% lower than the optimised cross-sectional area ( $N_{max} = 5$  in Fig. 5 (c)). Therefore, five flat segments per half cross-section likely represents an optimum number of segments for column lengths of 6.56 ft (2,000 mm).

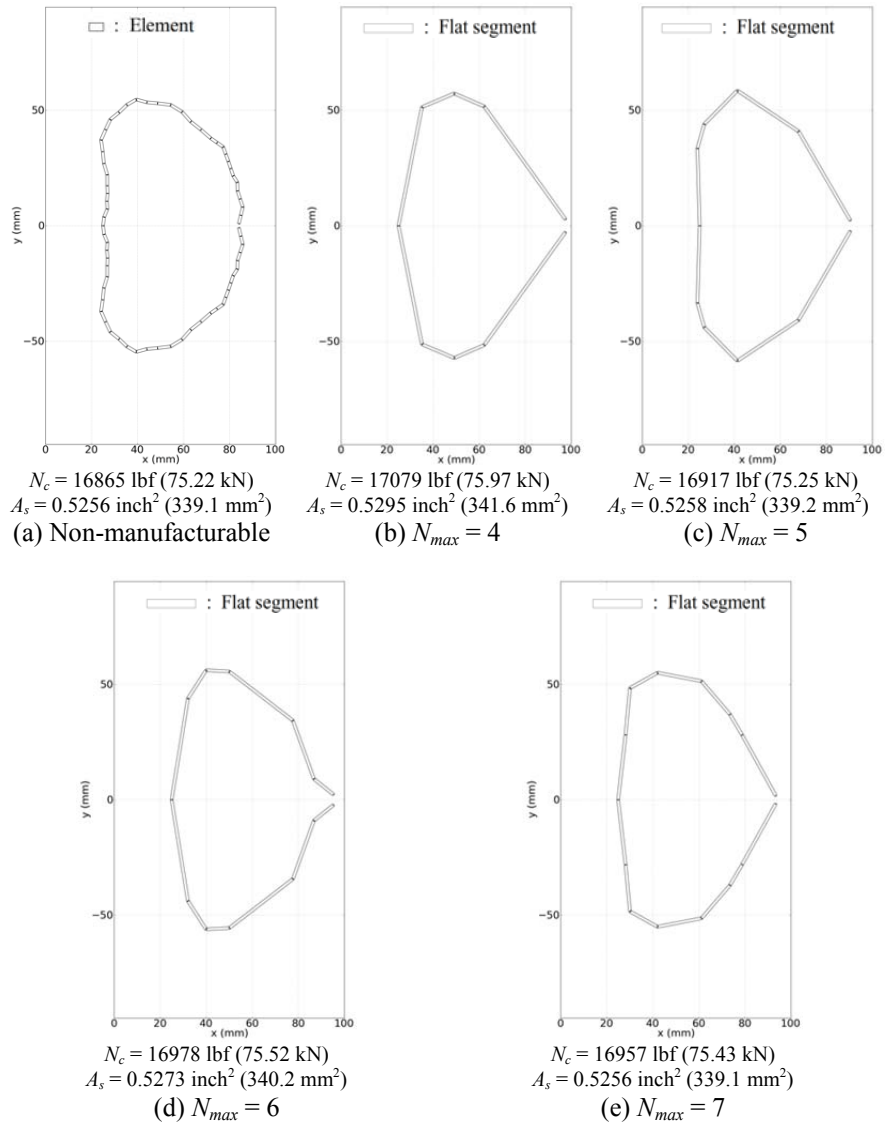


Fig. 5. Fittest optimised cross-sections for the 6.56 ft (2,000 mm) long columns at the final generation for (a) the non-manufacturable cross-section and (b) to (e)  $N_{max} = 4$  to 7

#### 4.4. Column length of 9.84 ft (3,000 mm)

Similar to Figs 2 and 4, Fig. 6 depicts the average fitness functions  $f$  for the 9.84 ft (3,000 mm) long columns. When  $N_{max} = 5$  and 6, the flat segments are too long for the algorithm to correctly align the elements constituting the cross-section in the Hough transformation, and the algorithm encounters convergence issues. For the  $N_{max} > 6$  curves, the convergence trend seems to be similar.

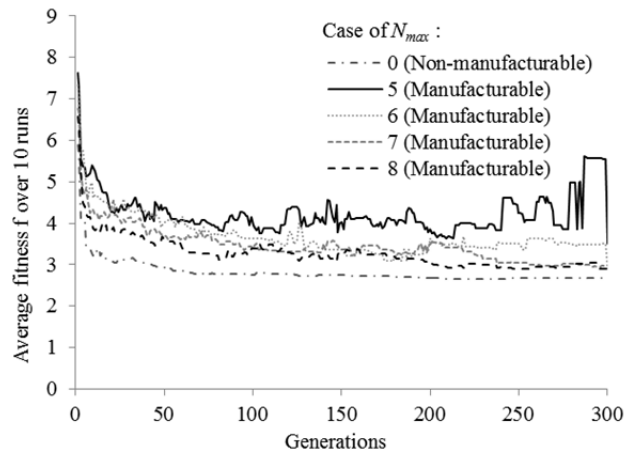


Fig. 6. Average fitness  $f$  for the 9.84 ft (3,000 mm) long columns

$N_{max}$	Cross-sectional area	Compression capacity			Alignment	
	$A_s$ (inch <sup>2</sup> (mm <sup>2</sup> ))	$N_c$ (lbf (kN))	Error <sup>(2)</sup> (%)	CoV	Error (%)	CoV
0 <sup>(1)</sup>	0.6843 (441.5)	16894 (75.15)	+0.20	0.0017	-	-
5	0.6398 (412.8)	16930 (60.63)	-19.16	0.2275	-1.3	0.0165
6	0.6797 (438.5)	16971 (73.14)	-2.47	0.1082	-0.4	0.0090
7	0.6908 (445.7)	16870 (74.59)	-0.55	0.0197	0.0	0.0000
8	0.6960 (449.0)	16944 (75.53)	+0.46	0.0317	0.0	0.0000

<sup>(1)</sup>: Algorithm ran without manufacturing constraints (non-manufacturable cross-section)

<sup>(2)</sup>: Error when compared to 75 kN

Table 3. Average results over 10 runs for the 9.84 ft (3,000 mm) long columns

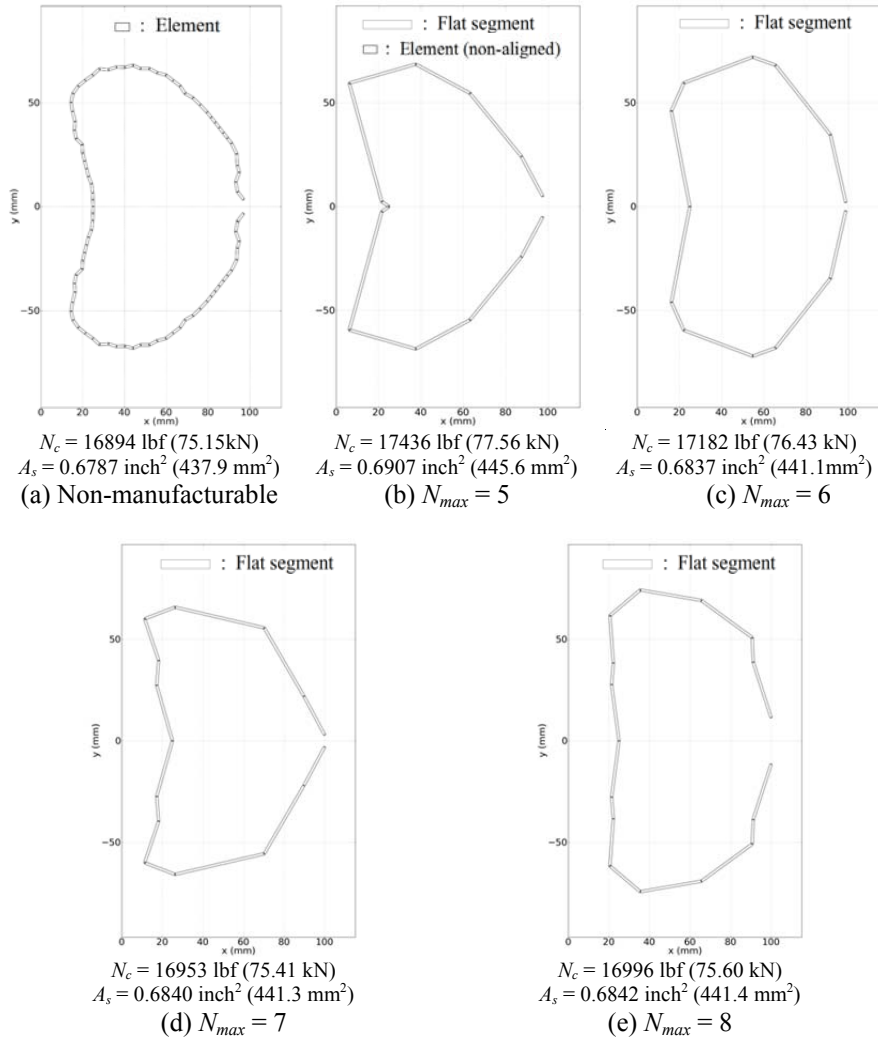


Fig. 7. Fittest optimised cross-sections for the 9.84 ft (3,000 mm) long columns at the final generation for (a) the non-manufacturable cross-section and (b) to (e)  $N_{max} = 5$  to 8

Table 3 summarises the average results over 10 runs. When the algorithm is run with manufacturing constraints, only  $N_{max} = 8$  achieves an average compressive axial capacity of at least 16,861 lbf (75 kN). Specifically, none, 5, 6 and 8 runs out of 10 satisfy all constraints when  $N_{max} = 5, 6, 7,$  and 8, respectively. For the

non-manufacturable cross-section, the constraint is satisfied for 9 runs out of 10. For large cross-sectional areas and low value of  $N_{max}$ , lower alignment penalty factors would be required in the AL to better explore the design space before convergence of the algorithm. When  $N_{max} = 8$ , the average cross-sectional area is  $0.6960 \text{ inch}^2$  ( $449.0 \text{ mm}^2$ ). This is 1.70% greater than the average optimised non-manufacturable cross-sectional area of  $0.6843 \text{ inch}^2$  ( $441.5 \text{ mm}^2$ ).

Fig. 7 plots the optimised fittest cross-sections at the 300<sup>th</sup> generation (final generation) out of 10 runs for each investigated case. The figure shows that all cross-sections, except for  $N_{max} = 8$ , tend to converge to a “ $\Sigma$ ” shape. These cross-sections have an overall depth of about 5.12 inch (130 mm). For  $N_{max} = 8$ , the cross-section converges more to a “bean” shape and has a larger overall depth of about 5.90 inch (150 mm). The fittest cross-section satisfying all constraints is given in Fig. 7 (c), i.e.  $N_{max} = 6$ , and has a cross-sectional area of  $0.6837 \text{ inch}^2$  ( $441.1 \text{ mm}^2$ ), i.e. 0.73% greater than the optimised non-manufacturable cross-sectional area of  $0.6787 \text{ inch}^2$  ( $437.9 \text{ mm}^2$ ), shown in Fig. 7 (a). Six flat segments per half cross-section would likely represent an optimum number of flat segments for column lengths of 9.84 ft (3,000 mm).

## 5. Future studies

As part of the future work, structural assembly constraints will be integrated into the algorithm allowing optimising both practical and manufacturable CFS cross-sections. Rules defined in Gilbert et. al. (2012a) considering all buckling modes, i.e. local, distortional and global buckling, will also be incorporated into the algorithm. Moreover, bending moment capacity of CFS members will be introduced into the algorithm to optimise the cross-sections to actual compressive and flexural loading patterns.

## 6. Conclusion

This paper has investigated the optimisation of manufacturable singly-symmetric open cross-sections of CFS columns for yielding and global buckling. Varying column lengths were analysed. The validated shape optimisation algorithm introduced in the companion paper is used for this purpose. For each column length, different numbers of flat segments per half cross-section are investigated and the optimum number of flat segments is discussed. This paper showed that introducing the manufacturing constraints into the algorithm increases the average cross-sectional area (over 10 runs) by up to 2% when compared to that of an optimised non-manufacturable cross-section.

**References**

- AS/NZS 4600, *Cold-formed steel structures*, Standards Australia, Sydney, Australia, 2005.
- Adeli H, Cheng N "Augmented Lagrangian Genetic Algorithm for Structural Optimization", *Journal of Aerospace Engineering*, 7, 104-118, 1994.
- Gilbert BP, Savoyat TJM, Teh LH "Self-shape optimisation application: Optimisation of cold-formed steel columns", *Thin-Walled Structures*, 60, 173-184, 2012a.
- Gilbert BP, Teh LH, Guan H "Self-shape optimisation principles: Optimisation of section capacity for thin-walled profiles", *Thin-Walled Structures*, 60, 194-204, 2012b.
- Wang B, Gilbert BP, Molinier AM, Guan H, Teh LH, "Shape optimisation of cold-formed steel profiles with manufacturing constraints: Part I Algorithm (companion paper)", *Proceedings of the 22nd International Specialty Conference on Cold-Formed Steel Structures*, St. Louis, Missouri, USA, 2014.